ChemComm

COMMUNICATION

View Article Online
View Journal | View Issue

Cite this: *Chem. Commun.*, 2014, **50**, 11358

Received 12th June 2014,
Accepted 23rd July 2014

DOI: 10.1039/c4cc04460f

www.rsc.org/chemcomm

Enhanced ratiometric fluorescent indicators for magnesium based on azoles of the heavier chalcogens†

Mohammad S. Afzal, Jean-Philippe Pitteloud and Daniela Buccella*

Red-shifted fluorescent indicators for magnesium were developed by incorporation of sulfur or selenium in the azole moiety of 'fura' fluorophores. Single atom replacement in the acceptor of these ITC probes affords longer excitation and emission wavelengths as well as greater separation between excitation bands, valuable for ratiometric intracellular Mg^{2+} imaging.

Fluorescent indicators are some of the most versatile tools for the study of the cell biology of metals, allowing for the rapid detection of ions with remarkable selectivity, sensitivity, and spatial resolution *via* fluorescence microscopy.[1,2] Wavelength ratiometric indicators are a class of probes that exhibit a change in excitation or emission wavelength upon interaction with an analyte, thus enabling the use of a ratio of intensities at two wavelengths as the readout.[3] In the context of biological imaging of metals, wavelength ratiometric indicators are particularly useful, as they provide quantitative information in a wide range of ion concentrations and sample matrices, with fluorescence outputs that are insensitive to uneven sensor concentration, photobleaching, and fluctuations in excitation intensity, among other external factors.[3,4] A number of ratiometric indicators display conjugated donor–acceptor structures that undergo photoinduced intramolecular charge transfer (ICT). Interaction of the metal cation with either donor or acceptor moieties may be employed to stabilize or destabilize the charge transfer state, thus affecting the excitation and emission wavelength.[5] The fura family of indicators[6,7] is a notable example of such a design applied to the detection of metal ions in biological samples. Fura-2[6] and its congener Furaptra[8] (commercially available as Mag-Fura-2), have been instrumental in the elucidation of numerous physiological and pathological roles of calcium and magnesium, respectively, despite various limitations associated with their short excitation and emission wavelengths. In the context of magnesium detection, significant progress has been made in the design of new generations of improved sensors.[9] Ratiometric indicators, however, remain scarce.

For live cell imaging, nontoxic dyes with high brightness and excitation and emission wavelengths in the visible range are desirable. Lower energy light minimizes sample damage, scattering, and background caused by autofluorescence.[1,2] Tuning the excitation or emission wavelength of indicators for fluorescence microscopy typically involves introducing significant changes in the structure of the fluorophores, which, for small-molecule indicators, often results in changes in their cellular uptake and localization properties. The ability to tune the photophysical features of a probe with minimal change of its structural and chemical properties is highly desirable. Sulfur and, to a lesser extent, selenium and tellurium have been exploited for the improvement of common organic luminophores,[10] affording compounds with longer absorption and emission wavelengths than their oxygen-containing counterparts. Furthermore, Moerner and coworkers recently reported the incorporation of selenium into an amino-D-luciferin scaffold, which led to a noticeable red shift in the bioluminescence of the compound with respect to the sulfur-based parent.[11] In our efforts to develop improved chemical tools for the study of biological magnesium, we surmised that the incorporation of heavier chalcogens into the structure of the Mag-fura-2 indicator would aid in shifting its excitation and emission to longer wavelengths, more amenable for live cell fluorescence imaging of Mg^{2+}. We demonstrate herein that strategic single atom replacement of the chalcogen in the acceptor oxazole moiety of this magnesium-responsive ICT indicator induces a large shift in emission wavelength and an increase in Stokes shift, without affecting significantly the essential chemical features of the compound. Most significantly, we show that the sulfur- and selenium-based dyes display greater separation between excitation maxima associated with their metal-free and metal-bound forms, a feature that becomes advantageous in ratiometric imaging.

For the incorporation of sulfur or selenium into the Mag-fura-2 structure, we prepared 2-methyl azoles **1a** and **1b** (Scheme 1) by cyclization of ethyl 2-chloro-3-oxopropanoate and either thioacetamide or freshly prepared selenoacetamide,[12] respectively.

Department of Chemistry, New York University, New York, NY 10003, USA. E-mail: dbuccella@nyu.edu

† Electronic supplementary information (ESI) available: Supporting figures, full experimental details and crystallographic information files. CCDC 1007936 and 1007937. For ESI and crystallographic data in CIF or other electronic format see DOI: 10.1039/c4cc04460f

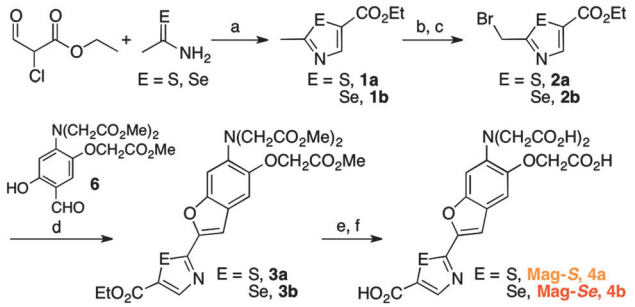

Scheme 1 Synthesis of indicators Mag-S and Mag-Se. Conditions: (a) MeCN, reflux; (b) 1,3-dibromo-5,5-dimethylhydantoin, AIBN, $AcOH_{(cat)}$, C_6H_5Cl–CCl_4, 75 °C; (c) $HPO(OEt)_2$, $^iPr_2EtN$, THF, 0 °C; (d) K_2CO_3, DMF, 100 °C; (e) KOH, MeOH–H_2O; (f) HCl or buffer pH 7.

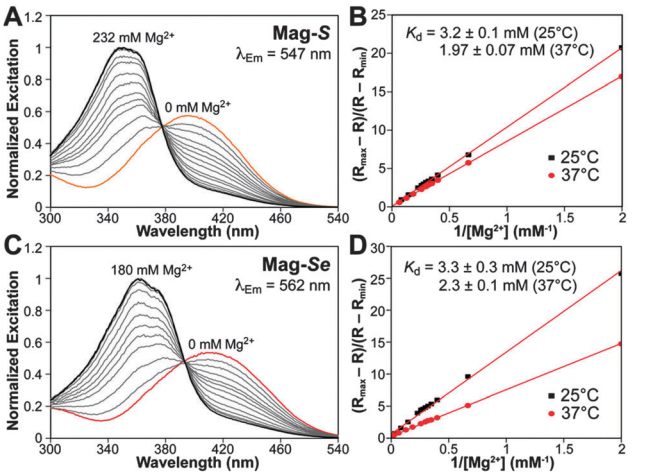

Fig. 1 Fluorescence excitation spectra of 2 μM solutions of Mag-S (A) and Mag-Se (C) with increasing concentrations of $MgCl_2$ (50 mM PIPES, 100 mM KCl, pH 7.0, 25 °C). Double reciprocal plots (B) and (D) show the dependence of the emission ratio on Mg^{2+} concentration for Mag-S and Mag-Se, respectively.

Subsequent unselective radical bromination led to mixtures of 2-bromomethylazole and 2-dibromomethylazole products. Treatment of the mixtures with diethylphosphite and Hünig's base enabled conversion of the undesired *gem*-dibromo byproducts to afford pure 2-bromomethylazoles **2a,b**.[13] These precursors were employed for the final assembly of the benzofuran fluorophores *via* condensation with salicylaldehyde **6**,[8] bearing the protected magnesium-binding moiety. The solid-state structure of the resulting dyes in their ester form was determined by single crystal X-ray diffraction, as shown in Fig. S12 (ESI†). Metal responsive sensors Mag-S and Mag-Se in the free acid form may be obtained *via* base-catalyzed hydrolysis of the esters. The deprotected *o*-aminophenol-*N,N*-triacetic acid (APTRA) group, however, is susceptible to degradation in acidic solutions. Accordingly, we chose to store the sensors in their more stable ester forms; stock solutions of the free acids for photophysical characterization were prepared by quantitative hydrolysis followed by neutralization *via* dilution into aqueous buffer right before use.

Photophysical properties of the new indicators were studied in aqueous buffer at pH 7.0, as summarized in Table 1 and Fig. S1 (ESI†). The thiazole derivative, Mag-S, displays an excitation maximum at 392 nm, with emission at 572 nm ($\Phi_{392} = 0.17 \pm 0.01$) in the metal-free form. The selenazole analogue Mag-Se shows an excitation maximum at 410 nm, with emission maximum at 584 ($\Phi_{410} = 0.09 \pm 0.02$) in the free state. Thus, a single replacement of O by Se in the structure of the fluorophore affords a greater than 70 nm bathochromic shift in the emission of the indicator. The lower fluorescence quantum yield of Mag-Se compared to that of the lighter chalcogen counterparts is likely due to a greater rate of intersystem crossing to a triplet state.[14,15] Large Stokes shifts in polar solvents are typical of fluorophores based on ICT. In the case of Mag-S and Mag-Se, the Stokes shifts are very large, reaching ~200 nm in the metal-saturated state and in general ~30 to 40 nm larger than those of Mag-fura-2.

Both Mag-S and Mag-Se compounds respond to Mg^{2+} showing a significant blue shift in the fluorescence excitation and emission spectra (Fig. 1), consistent with a destabilizing effect of the cation on an excited state characterized by a large dipole moment. The appearance of two distinguishable excitation bands makes the indicators suitable for excitation-ratiometric determination of magnesium in solution. The dissociation constants for 1 : 1 indicator-to-metal stoichiometry complexes at 25 and 37 °C were determined from linear fits of the intensity ratios, yielding low millimolar values (Mag-S $K_{d,Mg^{2+}} = 3.2 \pm 0.1$ mM; Mag-Se $K_{d,Mg^{2+}} = 3.3 \pm 0.3$ at 25 °C, Table 1) close to those of the parent Mag-fura-2 and well in tune with typical intracellular free magnesium concentrations.[16,17] Remarkably, the separation between excitation bands for the metal-free and -bound sensors based on the electron poorer thiazole and selenazole is larger than that of the oxazole derivative. This observation is indicative of the heavier chalcogen exerting a greater influence in stabilizing the excited state of the metal-free dye than the locally excited state of the metal-bound form. This feature is desirable for ratiometric imaging; as the separation between bands increases and their overlap is reduced, a greater portion of each band may be excited using wider excitation filters, thus increasing

Table 1 Photophysical properties of new sensors Mag-S and Mag-Se,[a] compared to oxazole analogue Mag-fura-2

	Absorption λ_{max} (nm), $\varepsilon \times 10^3$ (M^{-1} cm^{-1})		Excitation λ_{max} (nm)		Emission λ_{max} (nm), Φ^b		$K_{d,Mg^{2+}}$ (mM)		$K_{d,Ca^{2+}}$ (μM)	
	Unbound	Mg^{2+}-saturated	Unbound	Mg^{2+}-saturated	Unbound	Mg^{2+}-saturated	25 °C	37 °C	25 °C	37 °C
Mag-fura-2	369, 22[c]	330, 24[c]	370[d]	335[d]	511,[c] 0.24[d]	491,[c] 0.30[d]	1.9[c]	1.5[d]	25[c]	—
Mag-S	396, 29.1(7)	350, 30(1)	392	347	572, 0.17(1)	547, 0.30(1)	3.2(1)	1.97(7)	38(1)	35.3(7)
Mag-Se	412, 26.6(8)	360, 28.3(9)	410	361	584, 0.09(2)	562, 0.18(1)	3.3(3)	2.3(1)	41(2)	37.0(5)

[a] Measurements performed in 50 mM PIPES, 100 mM KCl, pH 7.0 at 25 °C unless otherwise indicated. [b] Quinine sulfate in 0.5 M H_2SO_4 ($\Phi_{347} = 0.546$)[18] was employed as a fluorescence standard. [c] Properties reported at 22 °C, from ref. 7. [d] From ref. 8.

the overall signal without compromising the selective excitation of the free and metal-saturated forms of the dye (*i.e.* minimal cross-talk between excitation channels).

We evaluated the fluorescence emission of the new compounds in response to various other biologically relevant metal ions including Ca^{2+}, Zn^{2+} and the first row transition metals from Mn^{2+} to Cu^{2+} (Fig. S2 and S3, ESI†). The metal selectivity of the Mag-S and Mag-Se probes is comparable to that of other reported APTRA-based metal ion indicators.[7] The fluorescence ratio is insensitive to low micromolar concentrations of most ions tested, with the exception of Zn^{2+} (Mag-S $K_{d,Zn^{2+}} = 62 \pm 3$ nM; Mag-Se $K_{d,Zn^{2+}} = 60 \pm 10$ nM at 25 °C).[19] Absolute fluorescence intensity values, however, show a decrease in the presence of the paramagnetic transition metals, thus implying some degree of binding that leads to quenching of the fluorescence. Despite this effect, the typical low concentrations of these trace metals in biological samples, and the negligible impact of their presence on the fluorescence ratio, suggests they would cause little interference in magnesium detection. In the case of calcium, a change in the fluorescence ratio is observed in the mid-micromolar concentration range. The new sensors may be, therefore, applied as low affinity calcium indicators (Mag-S $K_{d,Ca^{2+}} = 38 \pm 1$ μM and Mag-Se $K_{d,Ca^{2+}} = 41 \pm 2$ μM at 25 °C, Table 1) for the detection of high Ca^{2+} concentrations such as those associated with calcium fluxes.

Taking into consideration the superior brightness of the sulfur-containing indicator over the selenium analogue, we chose to test the response of Mag-S for the ratiometric detection of Mg^{2+} in live cells. To facilitate cellular uptake, the negatively charged carboxylates were masked as acetoxymethyl esters.[20] HeLa cells were loaded with 2 μM of the membrane-permeable dye, followed by washing and an additional 25 min incubation period to allow for the full de-esterification of the probe by intracellular esterases. Live cells were then imaged using a custom ratiometric filter set (see ESI† for details), capturing fluorescence emission above 500 nm (Fig. 2). The absolute intensity images captured for each excitation channel (Fig. S13, ESI†) reveal a relatively even staining of the entire cell, with little evidence for dye compartmentalization. The ratio image (Fig. 2B), more clearly shows the differences in magnesium levels in various intracellular compartments, with lower levels in the nucleus compared to surrounding organelles. To confirm the responsiveness of the indicator to Mg^{2+}, the imaging medium was supplemented with non-fluorescent ionophore 4-bromo-A-23187 (Molecular Probes) and 30 mM of $MgCl_2$ for 60 min before capturing a second set of images. A clear increase (~17%) in the average fluorescence ratio per cell was observed (Fig. 2D and E), in response to the increase in intracellular free Mg^{2+} mediated by the ionophore.

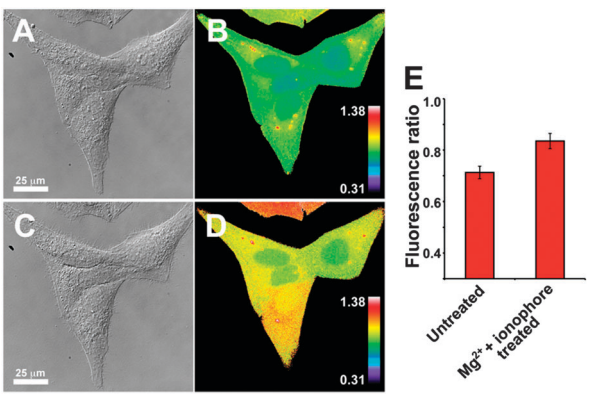

Fig. 2 Fluorescence imaging of intracellular free magnesium in live HeLa cells treated with 2 μM Mag-S acetoxymethyl ester before (A, B) and after (C, D) 60 min incubation with 2.5 μM magnesium ionophore 4-bromo-A-23187 and 30 mM exogenous $MgCl_2$. (A, C) DIC images; (B, D) fluorescence ratio images. Scale bars represent fluorescence ratio. (E) Change in the average fluorescence ratio per cell, reflecting an increase in intracellular magnesium upon treatment with exogenous Mg^{2+} and ionophore. Error bars = standard error of the mean, $N = 11$.

In summary, we have synthesized and characterized a new set of red-shifted ratiometric indicators for biological magnesium based on modified 'fura' fluorophores. The new compounds illustrate how the heavier chalcogens sulfur and selenium may be exploited to enhance the properties of fluorophores beyond the realm of fluorescence tags and labels, but also to enhance the properties of ion responsive fluorescent indicators. The replacement of the chalcogen in the azole acceptor group of the fura ICT dye, remote from the metal binding moiety, induces significant changes in the photophysical properties of the indicators with little impact in metal selectivity, dissociation constants, and cellular uptake properties that are essential for intracellular ion detection. Significantly, the 2-oxazolyl substituted 6-aminobenzofuran is the fluorescent core for various ion-selective fluorescent probes, not only for detection of Mg^{2+} and of Ca^{2+}, but also functionalized with metal-chelating groups specific for Zn^{2+} (FuraZin[21] and ZnAF-R2[22]), and for Na^+ (SBFO[23] and related crown ether-based indicators[24]). The chalcogen replacement strategy described herein may, therefore, open the doors to enhanced red-shifted ratiometric detection for other biologically relevant ions.

This work was supported by start-up funds from NYU to D. B. The authors thank Mr. Guangqian Zhang for fluorophore precursors. The Bruker AXS SMART APEXII Diffractometer was acquired through the support of the Molecular Design Institute at NYU. Bruker Avance-400 and 500 NMR Spectrometers were acquired with support of the NSF under award number CHE-01162222.

Notes and references

1 K. P. Carter, A. M. Young and A. E. Palmer, *Chem. Rev.*, 2014, **114**, 4564–4601.
2 D. W. Domaille, E. L. Que and C. J. Chang, *Nat. Chem. Biol.*, 2008, **4**, 168–175.
3 J. R. Lakowicz, *Principles of Fluorescence Spectroscopy*, Kluwer Academics/Plenum, New York, 2nd edn, 1999.
4 A. Demchenko, *J. Fluoresc.*, 2010, **20**, 1099–1128.
5 B. Valeur and I. Leray, *Coord. Chem. Rev.*, 2000, **205**, 3–40.
6 G. Grynkiewicz, M. Poenie and R. Y. Tsien, *J. Biol. Chem.*, 1985, **260**, 3440–3450.
7 R. P. Haugland, *Handbook of Fluorescent Probes and Research Products*, Molecular Probes Inc., Eugene, Oregon, 9th edn, 2002.
8 B. Raju, E. Murphy, L. A. Levy, R. D. Hall and R. E. London, *Am. J. Physiol.: Cell Physiol.*, 1989, **256**, C540–C548.
9 For recent examples of indicators for fluorescence imaging of Mg^{2+}, see: (*a*) T. Fujii, Y. Shindo, K. Hotta, D. Citterio, S. Nishiyama, K. Suzuki and K. Oka, *J. Am. Chem. Soc.*, 2014, **136**, 2374–2381; (*b*) C. Marraccini, G. Farruggia, M. Lombardo, L. Prodi, M. Sgarzi, V. Trapani, C. Trombini, F. I. Wolf, N. Zaccheroni and S. Iotti, *Chem.*

Sci., 2012, **3**, 727–734; (*c*) L. H. Lindenburg, J. L. Vinkenborg, J. Oortwijn, S. J. A. Aper and M. Merkx, *PLoS One*, 2013, **8**, e82009; (*d*) X. Dong, J. H. Han, C. H. Heo, H. M. Kim, Z. Liu and B. R. Cho, *Anal. Chem.*, 2012, **84**, 8110–8113; (*e*) Y. Zhao, B. Zheng, J. Du, D. Xiao and L. Yang, *Talanta*, 2011, **85**, 2194–2201; (*f*) Y. Shindo, T. Fujii, H. Komatsu, D. Citterio, K. Hotta, K. Suzuki and K. Oka, *PLoS One*, 2011, **6**, e23684; (*g*) V. Trapani, G. Farruggia, C. Marraccini, S. Iotti, A. Cittadini and F. I. Wolf, *Analyst*, 2010, **135**, 1855–1866.

10 For examples, see: (*a*) H. Takechi, Y. Oda, N. Nishizono, K. Oda and M. Machida, *Chem. Pharm. Bull.*, 2000, **48**, 1702–1710; (*b*) M. R. Detty, P. N. Prasad, D. J. Donnelly, T. Ohulchanskyy, S. L. Gibson and R. Hilf, *Bioorg. Med. Chem.*, 2004, **12**, 2537–2544; (*c*) B. Calitree, D. J. Donnelly, J. J. Holt, M. K. Gannon, C. L. Nygren, D. K. Sukumaran, J. Autschbach and M. R. Detty, *Organometallics*, 2007, **26**, 6248–6257; (*d*) M. J. Rose and P. K. Mascharak, *Inorg. Chem.*, 2009, **48**, 6904–6917; (*e*) M. W. Kryman, G. A. Schamerhorn, J. E. Hill, B. D. Calitree, K. S. Davies, M. K. Linder, T. Y. Ohulchanskyy and M. R. Detty, *Organometallics*, 2014, **33**, 2628–2640.

11 N. R. Conley, A. Dragulescu-Andrasi, J. Rao and W. E. Moerner, *Angew. Chem., Int. Ed.*, 2012, **51**, 3350–3353.

12 K. Geisler, W.-D. Pfeiffer, A. Künzler, H. Below, E. Bulka and P. Langer, *Synthesis*, 2004, 875–884.

13 P. Liu, Y. Chen, J. Deng and Y. Tu, *Synthesis*, 2001, 2078–2080.

14 M. R. Detty and P. B. Merkel, *J. Am. Chem. Soc.*, 1990, **112**, 3845–3855.

15 T. Y. Ohulchanskyy, D. J. Donnelly, M. R. Detty and P. N. Prasad, *J. Phys. Chem. B*, 2004, **108**, 8668–8672.

16 A. M. P. Romani, *Arch. Biochem. Biophys.*, 2011, **512**, 1–23.

17 R. D. Grubbs, *BioMetals*, 2002, **15**, 251–259.

18 A. M. Brouwer, *Pure Appl. Chem.*, 2011, **83**, 2213–2228.

19 The oxazole analogue, Mag-fura-2, binds Zn^{2+} with apparent K_d of 20 nM and has been employed for ratiometric measurement of Zn^{2+} in the mid to high nanomolar range. See: T. J. B. Simons, *J. Biochem. Biophys. Methods*, 1993, **27**, 25–37.

20 R. Y. Tsien, *Nature*, 1981, **290**, 527–528.

21 K. R. Gee, Z. L. Zhou, D. Ton-That, S. L. Sensi and J. H. Weiss, *Cell Calcium*, 2002, **31**, 245–251.

22 S. Maruyama, K. Kikuchi, T. Hirano, Y. Urano and T. Nagano, *J. Am. Chem. Soc.*, 2002, **124**, 10650–10651.

23 A. Minta and R. Y. Tsien, *J. Biol. Chem.*, 1989, **264**, 19449–19457.

24 V. V. Martin, A. Rothe, Z. Diwu and K. R. Gee, *Bioorg. Med. Chem. Lett.*, 2004, **14**, 5313–5316.